sine oculis Is a Homeobox Gene Required for Drosophila Visual System Development

Michelle A. Serikaku and Joseph E. O'Tousa

Department of Biological Sciences, University of Notre Dame, Notre Dame, Indiana 46556

Manuscript received May 2, 1994
Accepted for publication August 9, 1994

ABSTRACT

The so^{mda} (*sine oculis-medusa*) mutant is the result of a *P* element insertion at position 43C on the second chromosome. so^{mda} causes aberrant development of the larval photoreceptor (Bolwig's) organ and the optic lobe primordium in the embryo. Later in development, adult photoreceptors fail to project axons into the optic ganglion. Consequently optic lobe development is aborted and photoreceptor cells show age-dependent retinal degeneration. The *so* gene was isolated and characterized. The gene encodes a homeodomain protein expressed in the optic lobe primordium and Bolwig's organ of embryos, in the developing adult visual system of larvae, and in photoreceptor cells and optic lobes of adults. In addition, the SO product is found at invagination sites during embryonic development: at the stomadeal invagination, the cephalic furrow, and at segmental boundaries. The mutant so^{mda} allele causes severe reduction of SO embryonic expression but maintains adult visual system expression. Ubiquitous expression of the SO gene product in 4–8-hr embryos rescues all so^{mda} mutant abnormalities, including the adult phenotypes. Thus, all deficits in adult visual system development and function result from failure to properly express the *so* gene during embryonic development. This analysis shows that the homeodomain containing SO gene product is involved in the specification of the larval and adult visual system development during embryogenesis.

THE extensive analysis of adult visual system development in Drosophila has been useful in dissecting such processes as cell fate determination and pattern formation (for reviews see READY 1989; RUBIN 1991). During the third instar larval period, the developing adult photoreceptor cells of the eye-antennal imaginal disc project axons through the optic stalk which trigger development of the optic lobes (STELLER *et al.* 1987; KUNES *et al.* 1993). Establishment of this photoreceptor synapse is also necessary for maintenance of photoreceptor cells during the adult stage (CAMPOS *et al.* 1992). The larval visual system consists of two bilaterally positioned bundles of 12 photoreceptor cells called Bolwig's organ (BOLWIG 1946). These larval photoreceptors project axons that fasiculate to form Bolwig's nerve. Bolwig's nerve synapses with target cells in the cortex of the brain during late embryonic development to establish the larval visual system (TIX *et al.* 1987). Earlier in embryonic development, Bolwig's organ, the adult eye antennal disc, and the presumptive optic lobes originate from the same ectodermal invagination in the embryo (GREEN *et al.* 1993). Thus, the initial events of the specification of both the adult and larval visual system are related.

Previous work showed the *so* gene plays a role in the development of the adult eye. Homozygous so^{1} adults show a loss of compound eyes and ocelli and so^{2} flies have compound eyes that are relatively normal or only slightly reduced but still lack ocelli (HEITZLER *et al.* 1993). In this paper, we describe so^{mda}, a new class of *so* mutants, that in contrast to so^{1} and so^{2}, always have ocelli and produce relatively full-sized compound eyes. Our results suggest that *so* plays a critical role during embryonic development to establish both the larval and the adult visual system. We have cloned the *so* gene and show that it encodes a homeodomain protein expressed in the larval and adult visual systems as well as other sites in the embryo.

MATERIALS AND METHODS

Genetic analysis of so^{mda}: The so^{mda} mutant stock was generated in an *P* element germ-line transformation experiment. so^{mda} flies carry a single *P* element marked with ry^{+} and $ninaE^{+}$ genes on the right arm of chromosome *2* at position 43C. The *P* element was destabilized by mating so^{mda} flies to flies carrying a stable source of Δ2-3 transposase (ROBERTSON *et al.* 1988). Loss of the *P* element was monitored by a loss of the ry^{+} eye color. Five independent lines were generated from this dysgenic cross: three lines that are homozygous viable and two that are homozygous lethal.

Alleles of the lethal complementation groups and deficiencies at 43° were obtained from M. ASHBURNER to obtain a genetic map of the area. Deficiency stocks tested that uncover the *so* mutation were $Df(2R)Dr1^{R+21}$, $Df(2R)Dr1^{R+22}$, $Df(2R)Dr1^{R+28}$, $Df(2R)Dr1^{R+30}$, and Df(2R)NCX9. Stocks tested that did not uncover the *so* mutation were Df(2R)NCX5, Df(2R)NCX13, $l(2)43Ba^{Ew1}$, $l(2)43Ba^{Ew8}$, and $l(2)43Ba^{Ew11}$, $l(2)43Ba^{Ew15}$. See HEITZLER *et al.* (1993) for description of stocks.

The *P* element in the so^{mda} genome was localized to polytene chromosomes using standard techniques. Biotinylated DNA probes were made by nick translation using biotinylated Bio-16-dUTP. Preparation of slides, hybridization and signal

detection (strepavidin-conjugated horseradish peroxidase (HRP)/diaminobenzidine) were carried out according to Laverty and Lim (ASHBURNER 1989).

Assaying the mutant phenotype: All mutant phenotype analyses were done using the original *P* element allele of so^{mda}. To obtain light level sections of whole heads fly heads were fixed in Carnoy's solution for 4 hr. After three ethanol washes of 30 min each, heads were placed in 1:1 xylene/EtOH for 30 min, 100% xylene for 30 min and embedded in 3:1, 1:1 xylene:Polybed 812 for 30 min each. Heads were then embeded in 100% Polybed 812 overnight at room temperature. The next day heads were placed in blocks containing fresh Polybed 812 and hardened at 35° overnight, 45° the next day, and 60° overnight. One-micrometer sections were cut.

To study ultrastructure of the so^{mda} mutant adult eye, heads were bisected and fixed for transmission electron microscopy as previously described by READY (1989) with some modifications. Eyes were fixed in 0.75 M Na-cacodylate, 2% paraformaldehyde, 2% glutaraldehyde for 4 hr. Eyes were then fixed in above mixture plus 1% tannic acid at 4° overnight. The next day, three 10-min washes were done in 0.1 M Na-cacodylate. Post fixation was in 2% osmium tetraoxide in 0.1 M Na-cacodylate for 2 hr. The eyes were then washed again three times in H_2O and dehydrated in an ethanol series, treated with 1:1 xylene/EtOH for 30 min, 100% xylene for 30 min, and then treated with the Polybed 812 series as stated above.

Heads were fixed and post fixed for scanning electron microscopy (SEM) as stated above and then left in 70% ethanol overnight. The next day heads were further dehydrated in 80%, 95%, and 3 times 100% ethanol and then critical point dried and mounted for SEM. Embryos were fixed for SEM in an equal volume of heptane and 4% formaldehyde in phosphate buffer and post-fixed in osmium tetraoxide. Embryos were then dehydrated and prepared for SEM as stated above.

To assay the mutant physiological phenotype flies were immobilized on coverslips with wax and electroretinogram (ERGs) were measured using techniques previously described (LARRIVEE *et al.* 1981). The light stimulus pattern consisted of unattenuated orange and blue light stimuli. The flash remained on for 5 sec with a 25-sec interval between flashes.

Isolation of the *so* gene: To recover DNA sequences flanking the *P* element in the so^{mda} genome, we made a so^{mda} genomic phage library using the EMBL4 λ phage and the Gigapack Plus λ packaging kit (Strategene). Phage plaques were screened using a random primed ^{32}P-labeled probe containing *P* element sequences from plasmid 6.1 (RUBIN and SPRALDING 1982). Isolation of wild-type genomic and cDNA clones were done in the same manner using the Maniatis wild-type library (MANIATIS *et al.*, 1978) and a head-specific adult cDNA library (ITOH *et al.* 1985), respectively. All DNA sequences were determined using Sequenase Version 2.0 (U. S. Biochemical Corp.) and analyzed using the IBI Pustell Sequence Analysis software.

Expression of SO: To detect *so* RNA levels, we hybridized non-radioactive digoxigenin-labeled RNA probes (Boehringer Mannheim) to whole mount embryos of appropriate age. *In situ* hybridization was carried out according to TAUTZ and PFEIFLE (1989). Stained embryos were dehydrated in an ethanol series and mounted in 70% Permount/30% methyl salicylate.

To detect the SO protein, polyclonal antisera was generated against a SO fusion protein raised in mice. A 2.6-kb *Xho*I fragment of *so* cDNA6 sequences was ligated into the *Bam*HI site of pGEX3 (SMITH *et al.* 1986), after performing 2-bp fill-in reactions on both insert and vector. The fusion protein was purified from crude bacterial lysates by affinity chromatography using glutathione agarose beads according to SMITH and JOHNSON (1988).

For SO protein detection, appropriately aged embryos were collected and dechorionated with 50% bleach and then fixed in an equal volume of heptane and 4% formaldehyde in phosphate buffer. Subsequent steps were done according to ASHBURNER (1989) and the Vectastain ABC Elite kit (Vector Laboratories, Inc.). HRP stained embryos were dehydrated in an ethanol series, washed in methanol two times for 20 min and then washed in methyl salicylate overnight at room temperature. The next day, embryos were washed in methanol, ethanol, and xylene (3 × 20 min in each solvent), mounted in Permount, and viewed using Normarski optics.

Eye-antennal imaginal discs were fixed in PLP (2% paraformaldehyde, 0.01 M sodium *m*-periodate, 0.075 M lysine, and 0.035 M phosphate buffer) for 30 min, washed briefly and permeabilized in 0.5% Nonidet P-40 in PBT (10 mM $NaPD_4$, 130 mM NaCl, 0.1% Triton X-100, pH 7.6) for 30 min. Discs were then incubated in blocking buffer for 1 hr and then in primary antibody in PBT overnight at 4°. Subsequent steps were done using the Vectastain ABC Elite kit and labeled discs were mounted in glycerol.

To study expression patterns in adult eyes, eight micrometer sections were cut from frozen whole heads. The slides were air dried for 30 min. Tissue was fixed in 2% phosphate-buffered formalin for 30 min, rinsed for 5 min in TBS, and then incubated in antiserum diluted 1:250 in TBS for 30 min. The antiserum was then washed off in TBS (10 mM tris hydroxylmethyl aminomethane, 150 mM NaCl, pH 8.0) for 5 min and tissue was then incubated in fluorescein isothiocyanate goat-anti-mouse IgG diluted 1:50 in TBS for 20 min. After a final rinse for 5 min in TBS, coverslips were mounted on slides with 90% glycerol in TBS + 0.1% phenylenediamine.

Heat shock promoter plasmid construction and germ-line transformation: We placed the *so* cDNA 6 under the heat shock promoter, hsp70, in the vector pCaSper-hs (SCHNEUWLY *et al.* 1987) which carries the $white^+$ (w^+) gene. The entire *Eco*RI cDNA 6 fragment was ligated into the polylinker of the vector.

The so^{mda} stock (original *P* element allele stock homozygous for *w*) was injected with this construct and w^+ flies were selected. Germ-line transformants were then mated to w^+ *so* flies and resulting embryos were heat shocked at 37° for 1 hr and assayed for a rescue of the so^{mda} mutant pseudopupil phenotype. Flies with normal pseudopupils were prepared for light level sectioning and ERGs to document rescue of other aspects of the mutant phenotype.

RESULTS

The so^{mda} mutation is the result of a *P* element insertion: The so^{mda} mutation was generated in germ-line transformation experiments using an engineered *P* element vector. *In situ* hybridization showed that only one *P* element existed in the so^{mda} strain. The *P* element insertion maps to position 43C on the right arm of chromosome 2. The so^{mda} mutation also maps to this position as chromosomes containing deficiencies in the 43C region uncover the so^{mda} mutation (see MATERIALS AND METHODS). To show that the *P* element insertion was responsible for the so^{mda} mutation, the transposon was destabilized by mating homozygous so^{mda} flies to flies carrying a stable source of transposase. Two of three homozygous viable chromosomes recovered from this dysgenic cross possessed a reversion of so^{mda} to wild-type,

as assayed both by ultrastructural morphology and electroretinogram responses (data not shown). This confirms that the *P* element insertion causes the so^{mda} mutation. The third viable chromosome displayed a so^{mda} mutant (structural and physiological) phenotype of the same severity as the original so^{mda} mutation, suggesting that it resulted from an imprecise *P* element excision event that left the so^{mda} locus nonfunctional.

Complementation studies show that flies heterozygous for the so^{1} mutation and the so^{mda} mutation give a wild-type phenotype. However, a chromosome having a lethal at the 43C region was also generated from our *P* element excision crosses. This lethal failed to complement both so^{mda} and the severe allele, so^{1}, which also maps within the 43C region on chromosome 2 (HEITZLER *et al.* 1993). Additional work to be described in this report, as well as data to be reported elsewhere (CHEYETTE *et al.* 1994) confirms that so^{mda} is defective in the same transcription unit as *so*, hence the allele is described as so^{mda}.

so^{mda} mutation affects adult eye and brain structure: The external eye structure of so^{mda}, shown in Figure 1B, reveals that the peripheral regions of the eye shows indentations or depressions. The overall external morphology of individual ommatidial units appears normal, even within the indented regions at the perimeter of the eye (Figure 1C). The internal eye and brain structures of adult so^{mda} flies are also affected. Figure 1D is a frontal section of a wild type fly showing the highly organized patterns of the retina and optic lobes, which are separated by a uniform basement membrane. so^{mda} flies lack organized optic lobes (Figure 1E). The tissue occupying the space between the eye and the central brain is highly disorganized and does not appear to be neural in origin. The type and structure of the tissue mass found in these areas varies from fly to fly, and is typically different on the left and right sides of the same fly. so^{mda} flies also show an abnormal basement membrane. The underlying disorganized tissue invades the retina at basement membrane gaps. The flies shown in Figure 1 are 5 days of age; the same phenotype is seen in newly eclosed so^{mda} flies (data not shown).

Photoreceptors of so^{mda} flies exhibit severe defects in the light evoked response as measured by ERG recordings (Figure 1F). The wild-type response has a sustained response with an amplitude of approximately 25 mV and a transient component at the initiation and termination of the light stimulus. The sustained response is primarily due to photoreceptor depolarization, while the transient components are due to second order cells in the lamina, the first optic ganglion, responding to photoreceptor depolarization. Mutant so^{mda} flies show a drastic decrease in the sustained amplitude of the ERG and an absence of transient components. This phenotype is present at eclosion, before the retina has shown extensive degeneration.

Figure 2 shows the morphology of the retina in young and old so^{mda} flies. The photoreceptor cells of young one day old so^{mda} flies have normal morphology, although they typically contain rhabdomeres that are irregular in shape (Figure 2B). Occasionally, mutant ommatidial units show abnormal numbers of rhabdomeres or cell bodies. An extra cell body was detected in 3% (2/68) of ommatidia, and loss of a cell body was seen in 6% (4/68) of ommatidia. Photoreceptor cells lacking rhabdomeres were observed at the rate of 20%. Also present in the young retina are areas devoid of photoreceptor cells (data not shown). These likely represent regions in which the underlying tissue masses of the optic lobe region have invaded the retinal layer.

At 14 days of age, mutant flies show extensive photoreceptor degeneration throughout the retina, leaving few clusters of ommatidia that have recognizable structure (Figure 2, C and D). Of the cells that remain, many contain abnormal rhabdomere structures. Some cells completely lack microvillar membrane, and others contain rhabdomeres that are broken into multiple units. Photoreceptors within a single ommatidium can show these different rhabdomeric phenotypes, and the R7 and R8 central cells are affected to a similar degree as the outer R1–6 cells.

Molecular characterization of *so* gene: The *P* element "tag" disrupting the *so* locus allowed the *so* gene to be cloned by screening a so^{mda} mutant genomic phage library using *P* element sequences as a probe. DNA fragments isolated in the mutant library were then used to screen a wild-type library (MANIATIS *et al.* 1978). One of the identified wild-type clones was cytogenetically mapped to 43C on polytene salivary chromosomes, the original site of the so^{mda} *P*-element mutation (data not shown). cDNAs coded within this region were then isolated from a head-specific adult cDNA library (ITOH *et al.* 1985).

The DNA sequence of the cDNAs and corresponding regions of the genomic DNA was determined. This effort generated the molecular map of the *so* gene shown in Figure 3A. The *P* element responsible for the so^{mda} mutation is positioned 26 bases upstream of the start of the longest cDNA. Within our collection of five cDNAs, two vary from the consensus in notable ways. One shows an alternative splice at the 5′ end of the gene, producing a transcript that contains the same open reading frame but may have an alternative 5′ start site. The second variant has failed to splice out the genomic DNA corresponding to intron 3. Failure to splice this intron results in premature termination of the open reading frame, so this cDNA likely originated from an incompletely spliced mRNA (data not shown).

The SO protein contains a homeodomain coded in exons 3, 4 and 5. Figure 3B shows the alignment of this domain with one mouse and five Drosophila homeodomains. SO shares greatest overall homology with the Drosophila homeodomains Dpbx and ro (31% identity) and shows strongest localized homology within helix 3, the recognition helix of the helix-turn-helix motif.

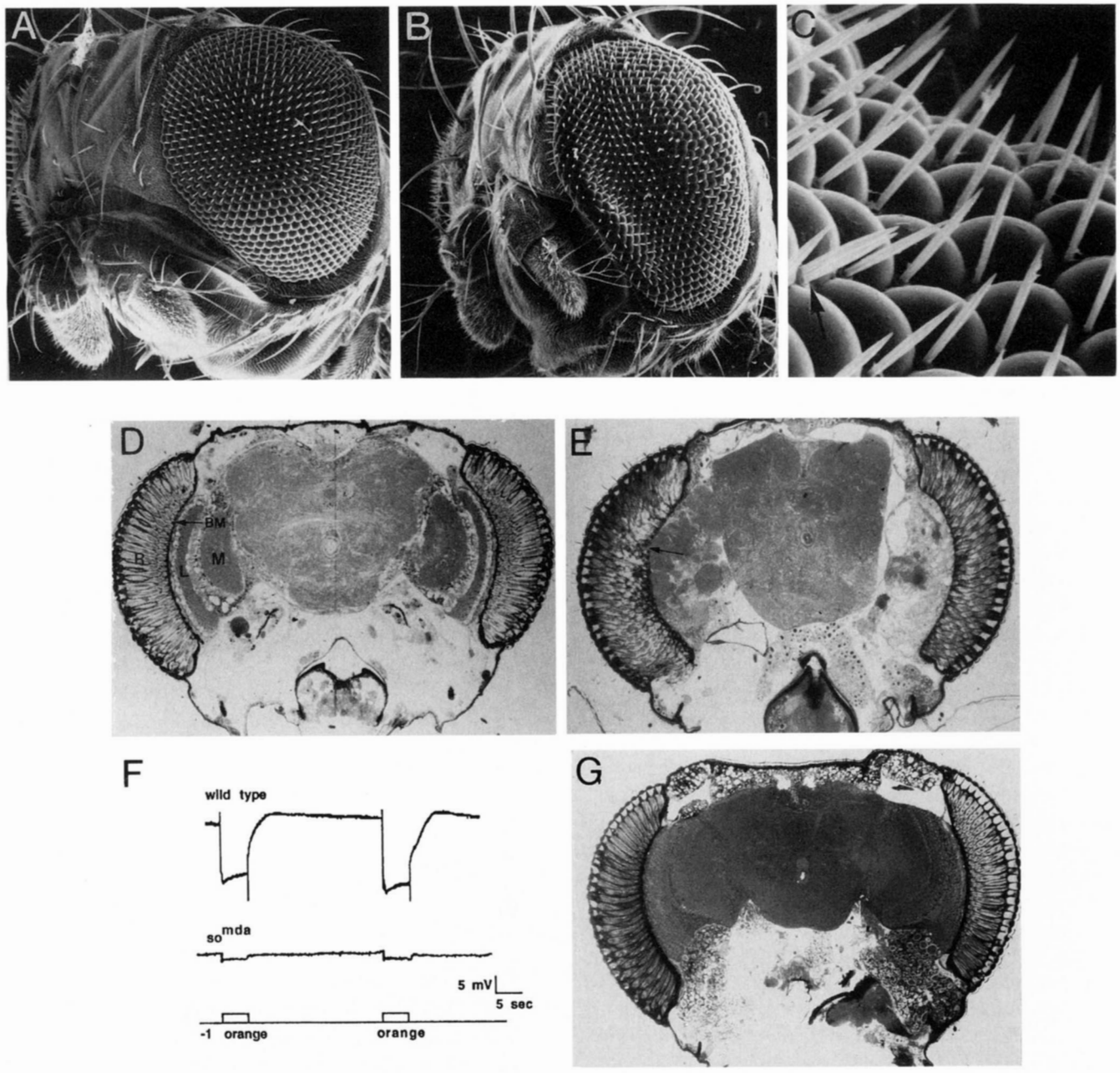

FIGURE 1.—Adult phenotypes of so^{mda}. (A) Scanning electron micrographs of wild-type eye shows a regular array of approximately 800 ommatidial units, with a single bristle located at the anterior margin of each unit. Magnification, 130×. (B) The so^{mda} eye displays a rough eye phenotype due to indentations at the margins of the eye. Magnification, 128×. (C) A higher magnification of a so^{mda} eye shows that the ommatidial units within the indented areas are normal in shape and size. One defect in the bristle pattern (arrow) is present. Magnification, 1420×. (D) Internal head structure of wild-type and so^{mda} (E) flies are shown (125×). The retina (R), basement membrane (BM), lamina (L) and medulla (M) are labeled in the wild-type micrograph. The so^{mda} head lacks organized optic lobe structures, and defects in the structure of the basement membrane are present (arrow). (F) Electroretinogram response of wild-type and so^{mda} retinas. Wild-type recording showing transient components at the initiation and cessation of the light response and a sustained amplitude of 25 mV. so^{mda} mutant recording lacks transient components and shows a drastic reduction in amplitude. (G) A 7-day-old transformed fly heat-shocked during embryogenesis shows normal optic lobe structures connecting the eyes to the central brain (125×).

Figure 4 shows the consensus cDNA sequence and the amino acids coded by the SO open reading frame. The first ATG initiation codon within the open reading frame was selected as the initiation codon because it is surrounded by a good match (5/7) to the Drosophila consensus sequence for translation initiation (CAVENER 1987). Analysis of the predicted 416-amino acid sequence indicates that the SO protein has an estimated molecular mass of 45 kilodaltons and is hydrophilic in nature. The sequence contains stretches of glutamine (opa) repeats (WHARTON *et al.* 1985), as well as glycine and alanine repeats, in its open reading frame.

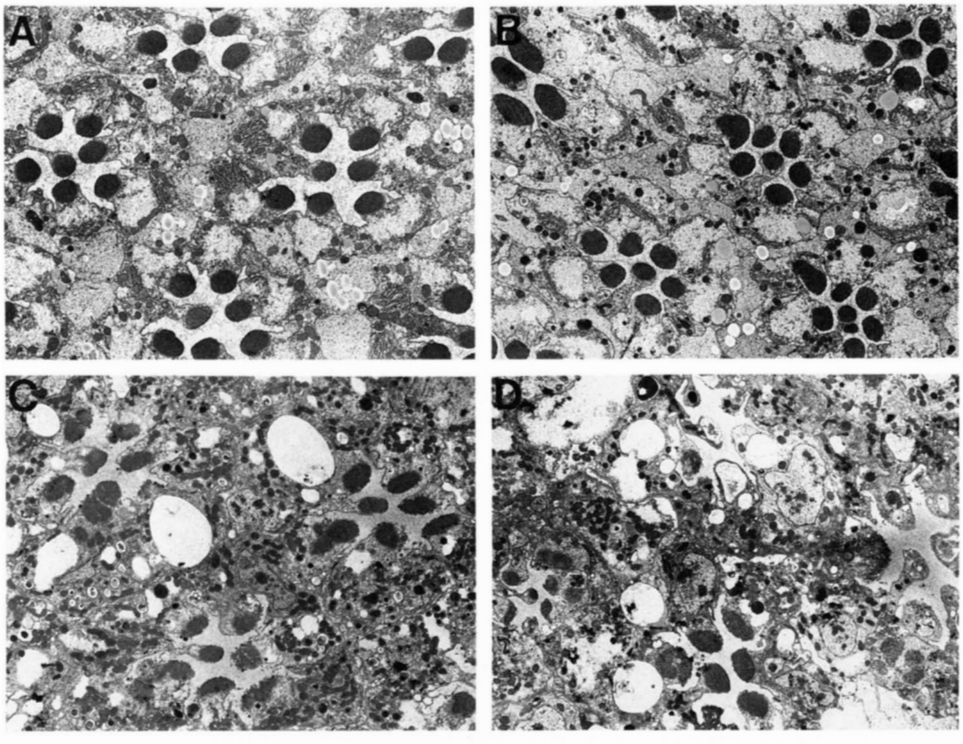

FIGURE 2.—Photoreceptor cell structure in wild-type and so^{mda} flies. Magnification, 2500×. (A) The 14-day-old wild-type retina shows the normal array of ommatidial units containing seven photoreceptor cells. (B) A young, 1-day-old so^{mda} retina typically has clusters containing seven photoreceptors with rhabdomeres that are small and abnormally shaped, but cells appear relatively healthy. (C and D) In the 14-day-old so^{mda} retina, many cells lack rhabdomeres and show other signs of degeneration.

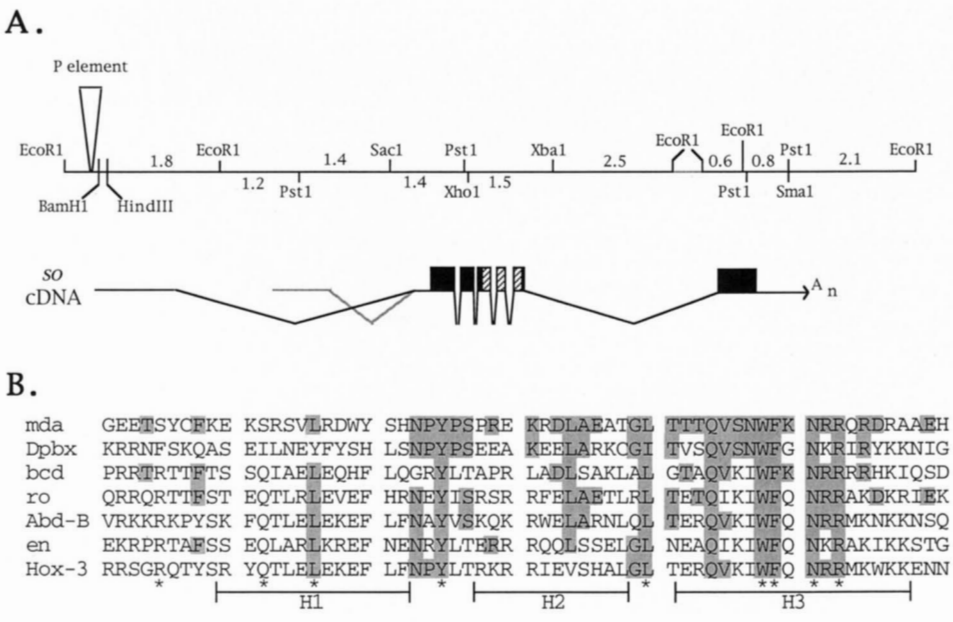

FIGURE 3.—*so* gene organization and homeodomain structure. (A) The *so* transcription unit spans over 13 kb of genomic DNA. The location of the exons and introns of the major cDNA form are shown in black lines. Another variant cDNA is shown in gray lines. The *P* element is located near the start site of the 5′-non-coding portion of the major cDNA class. The shaded boxes indicate the open reading frame and the cross-hatched boxes indicate the homeodomain encoded in exons 4, 5 and 6. (B) Comparison of the so homeodomain to other homeodomains. Sequences of the 61 amino acid homeodomain are compared. Dpbx (FLEGEL *et al.* 1993), bcd (DRIEVER and NUSSLEIN-VOLHARD 1989), ro (TOMLINSON *et al.* 1988), Abd-B (REGULSKI *et al.* 1985), and en (POOLE *et al.* 1985) are Drosophila proteins. Hox-3 (BREIER *et al.* 1988) is a mouse protein. Shaded amino acids indicate identical amino acids to the so homeodomain. Amino acids conserved in all known Drosophila homeodomains are indicated (*). The putative H2 and H3 helices form the helix-turn-helix motif critical for DNA binding.

Expression of SO in embryogenesis: SO is expressed at multiple stages during embryonic development. Tissue *in situ* hybridizations on whole-mount wild-type embryos (Figure 5) show that *so* is expressed in the optic lobe primordia immediately anterior to the cephalic furrow and in cells immediately anterior to the stomodeal invagination during germ band extension (stage 9). Later, in stage 12, *so* RNA is detected bilaterally at

```
GTTCTCAGTTGTTTTCGAGA TTCCGTCGCGTGCGGTTCGC TGCCCGTTCTACCCACGTCG CTCGCTTAGTAATCCAGGCC GGACCCGGCGGTCTTTCGAC  100
GTCCCGCGCACAAAGTTATA TTTAATTTGCGTGTTTCCTG AATGAACGCATCAGTATCGC GCCACATAAACGCACACGAA GCGAGAGAAAAGCGAGCAAA  200
ATTGAGCTAATCAATCCGCG GGCGGCCATTTTTTGTTGGC ACTGCCTCAGTGCTGTCGTC GCAGCTTTGCCCACCAAATT TGCAGGTGCAATTTGTCCGA  300
GTCGCGCAGGACAGCGAAGT TTTCGCGAAAAGTAATTTGC AACACGTGTTCGCACAGTGC GTATGAGCAATATTCAACGG CAAGCTTGTGTTAGTTAGTG  400
CCCAGTGTGATCGCGACTAA AAGTGTGTGCGTGCGCGAAC GGCACATGGCTTCGATTTGA AGAGTTTGGCCAAAATGCAA ATCAAGGAAATGCCGCACAG  500
CCGAAATCAGCGCCTTCTTG GCCAACTCTAACATTTGCGG ATATAGCACAAGTCGAATCG GAAAGCCAAGGCAAAAGGCA CAAACCCAAACAAAGAGTAA  600
                                                 GTGAGCAGC--4.0 kb-ATCATTGCAG
CAAACAAAAACTAACAAACT AGGATACGTATCAACAATAA ATAATCAAAATACAGCGCTC AAAACACCAAAGATTTAGGC AACTACTAGTTTAGGTTACA  700
CCATTCACCAGTTCAACTGA TCGATCCCTTCTGCAACTTG TAGCGGTGTCCTTGAAATCC ACCCCACCAACATCCAGCCA GGCAACCGATTCCCGCAGAA  800

A ATG TTA CAG CAT CCC GCC ACA GAT TTC TAC GAC TTG GCC GCG GCC AAT GCG GCT GCC GTT CTC ACC GCC CGT CAC ACG 879
  Met Leu Gln His Pro Ala Thr Asp Phe Tyr Asp Leu Ala Ala Ala Asn Ala Ala Ala Val Leu Thr Ala Arg His Thr

CCT CCT TAT AGT CCC ACC GGT CTC AGC GGA TCG GTG GCC CTG CAC AAC AAC AAC AAC AAT AAC AGC AGC ACC AGC AAT  957
Pro Pro Tyr Ser Pro Thr Gly Leu Ser Gly Ser Val Ala Leu His Asn Asn Asn Asn Asn Ser Ser Thr Ser Asn

AAC AAC AAC AGC ACT CTG GAC ATC ATG GCG CAC AAC GGC GGC GGA GCA GGC GGT GGC CTC CAT CTG AAC AGC AGC AGC 1035
Asn Asn Asn Ser Thr Leu Asp Ile Met Ala His Asn Gly Gly Gly Ala Gly Gly Gly Leu His Leu Asn Ser Ser Ser

AAC GGC GGC GGC GGC GGC GGA GTG GTC AGT GGT GGA GGC TCC GGC GGC AGG GAG AAC CTG CCC AGC TTC GGC TTC ACC 1113
Asn Gly Gly Gly Gly Gly Gly Val Val Ser Gly Gly Gly Ser Gly Gly Arg Glu Asn Leu Pro Ser Phe Gly Phe Thr
                          GTAATCACAA-135 bps-ACACCTACAG
CAG GAG CAG GTG GCC TGT GTT TGC GAG GTT CTC CAG CAG GCG GGC AAC ATC GAA AGA CTG GGC CGC TTC CTC TGG TCG 1191
Gln Glu Gln Val Ala Cys Val Cys Glu Val Leu Gln Gln Ala Gly Asn Ile Glu Arg Leu Gly Arg Phe Leu Trp Ser

CTG CCA CAA TGT GAT AAG CTG CAG CTG AAC GAG TCC GTG CTG AAG GCC AAG GCG GTC GTC GCA TTC CAC CGG GGA CAA 1269
Leu Pro Gln Cys Asp Lys Leu Gln Leu Asn Glu Ser Val Leu Lys Ala Lys Ala Val Val Ala Phe His Arg Gly Gln

TAC AAG GAG CTG TAC CGC CTG CTC GAG CAT CAC CAC TTC TCG GCC CAG AAT CAC GCC AAG CTC CAG GCC CTG TGG TTG 1347
Tyr Lys Glu Leu Tyr Arg Leu Leu Glu His His His Phe Ser Ala Gln Asn His Ala Lys Leu Gln Ala Leu Trp Leu
GTCAGCCTCC-135 bps-ACGACTGTAG
AAA GCG CAT TAT GTG GAA GCC GAA AAA CTG CGC GGA AGA CCC TTG GGT GCT GTT GGC AAA TAT CGT GTT CGC CGT AAA 1425
Lys Ala His Tyr Val Glu Ala Glu Lys Leu Arg Gly Arg Pro Leu Gly Ala Val Gly Lys Tyr Arg Val Arg Arg Lys
                                                 GTGAGTTCGG-0.2-1.0 Kb-TCATCCGCAG
TTT CCA TTG CCC CGC ACC ATC TGG GAT GGC GAG GAG ACG AGC TAC TGT TTT AAG GAA AAA TCG CGC TCC GTA CTG AGG 1503
Phe Pro Leu Pro Arg Thr Ile Trp Asp Gly Glu Glu Thr Ser Tyr Cys Phe Lys Glu Lys Ser Arg Ser Val Leu Arg

GAC TGG TAC TCG CAC AAT CCG TAT CCA TCG CCG CGG GAG AAA CGC GAT CTG GCC GAG GCC ACA GGA CTG ACC ACC ACG 1581
Asp Trp Tyr Ser His Asn Pro Tyr Pro Ser Pro Arg Glu Lys Arg Asp Leu Ala Glu Ala Thr Gly Leu Thr Thr Thr
GTGAGTCGAT-202 bps-GCTTTTACAG                                    GTGAGTTGCA-≥3.5 kb-TCCATTACCAG
CAG GTT TCC AAT TGG TTC AAG AAC CGA CGA CAA AGA GAT CGA GCT GCC GAA CAC AAA GAC GGC TCC ACG GAC AAG CAG 1659
Gln Val Ser Asn Trp Phe Lys Asn Arg Arg Gln Arg Asp Arg Ala Ala Glu His Lys Asp Gly Ser Thr Asp Lys Gln

CAC CTT GAC TCC TCC AGC GAC TCC GAG ATG GAG GGC AGC ATG TTG CCC AGC CAG AGT GCG CAG CAC CAG CAG CAG CAG 1737
His Leu Asp Ser Ser Ser Asp Ser Glu Met Glu Gly Ser Met Leu Pro Ser Gln Ser Ala Gln His Gln Gln Gln Gln

CAA CAG CAG CAG CAT TCA CCC GGC AAC AGC AGC GGC AAC AAC AAC GGC CTG CAT CAG CAG CAG CTG CAG CAT GTC GCC 1815
Gln Gln Gln Gln His Ser Pro Gly Asn Ser Ser Gly Asn Asn Asn Gly Leu His Gln Gln Gln Leu Gln His Val Ala

GCC GAG CAA GGC CTG CAG CAC CAT CCG CAC CAG CCA CAT CCC GCC AGC AAT ATC GCC AAT GTC GCC GCC ACC AAG AGC 1893
Ala Glu Gln Gly Leu Gln His His Pro His Gln Pro His Pro Ala Ser Asn Ile Ala Asn Val Ala Ala Thr Lys Ser

AGT GGC GGT GGC GGC GGA GGA GGC GTG AGT GCG GCG GCC GCT GCC CAG ATG CAA ATG CCT CCA CTG ACC GCC GCC GTG 1971
Ser Gly Gly Gly Gly Gly Gly Gly Val Ser Ala Ala Ala Ala Ala Gln Met Gln Met Pro Pro Leu Thr Ala Ala Val

GCC TAT TCG CAC CTG CAC AGC GTG ATG GGC GCC ATG CCC ATG ACC GCC ATG TAC GAC ATG GGC GAG TAC CAG CAC TTA 2049
Ala Tyr Ser His Leu His Ser Val Met Gly Ala Met Pro Met Thr Ala Met Tyr Asp Met Gly Glu Tyr Gln His Leu

TGA T TCTAGTT GGAGGCGGCCGCTGCCGCCG GTGGCACTGGCGGGGTCAGC GGCGGGGTCAGTGGCGGCAG CAGCAGCAGCTTGAGCGGCA        2140
***
GCAACATCGCCTTGCAGCAG CGACAACGCCACCAGCAGCA GCAGCAGTGCGAGAGCTTCT ACTTCTGAGGTGGTGGTTGG CCACCAAGCAATATCGCCGG 2240
ACTCCTTCGGCACAGCAGCA CAAACTTTACATATCGCCCG ATTGCTGGAAGGCTGTCATG AGTGGATATTCAGCTTCCAA ATGCTTGGCAAGGGGATTCT 2340
GGCTGGCGATCCGATGGAGA ACTACATGGCCCGGGAAACC ATATCAAACCGCAGTGGCAA TTGGGTCAGCCAACCCAGAA ATTCAAGTATCGGCCATGAC 2440
AGTATTTTAGCCAATTGCCG ATATGCCATTATAGCCCCAC ACTTTCCGGATAACATGGCA TTTCCGCAACCAGAGATAGA GATATATAGAATTGGAGCTG 2540
CAGCACAATCTCCTGGAAGG ATTCCAGGGGGAAACTATGA ACTTTCAACTATGACTTCTG CATCGATCTGTGTAAATAGC TAGGCTTTAGTTTTTAGTGC 2640
GGTTGGGAGGCCGACCGAAA TGCAAATCAAATCGAAACGT GCAAAAATTAAATGTAAACC TACGTACATGCATAAATTAT ACACTTTTAATTGTAGCCCC 2740
TAGTAATTCTATTTTTGTTA AAAATAAATTCTATTAAATT ATTTTCAAATGCAAAAAAAA                                          2800
```

FIGURE 4.—DNA sequence of the *so* transcript. The first ATG in the open reading frame starts at base 809 in the DNA sequence and extends for 416 amino acids. The deduced amino acid sequence is shown below the cDNA sequence. The *so* gene has 6 introns, shown with carats above the DNA sequence. Junction regions and available information on the sizes of the introns are indicated. The DNA sequence encoding the homeodomain is underlined.

segmental boundaries in a set of unidentified epidermal cells (Figure 5C). At stage 16, expression is limited to four bilaterally positioned organs at the anterior region of the head (Figure 5, D and E). Based on their position, the posterior, more heavily stained, organs likely correspond to Bolwig's organs. Antibody staining of wild-type embryos with antiserum generated against a SO fusion protein produced similar patterns of expression as the RNA expression at all stages of development. Figure 6A shows antibody staining at segmental boundaries in wild-type embryos at stage 12.

so^{mda} embryos, in contrast, do not show detectable levels of *so* RNA (Figure 5, F–H) or protein (Figure 6B) at any embryonic stage. This result suggests that the antiserum is specific for the SO protein, and demonstrates that SO embryonic expression is drastically reduced or absent in so^{mda} embryos.

Expression of SO in compound eye development: In wild-type eye discs, SO antisera stains nuclei on both sides of the morphogenetic furrow. Staining ahead of the furrow occurs within the undifferentiated cells of the eye disc epithelium. Posterior of the furrow, staining becomes restricted to individual photoreceptor cell clusters. Figure 7A shows the staining pattern in the wild-type eye disc. The developing R1–6 cells are more intensely labeled than the R7 cell (Figure 7C). The

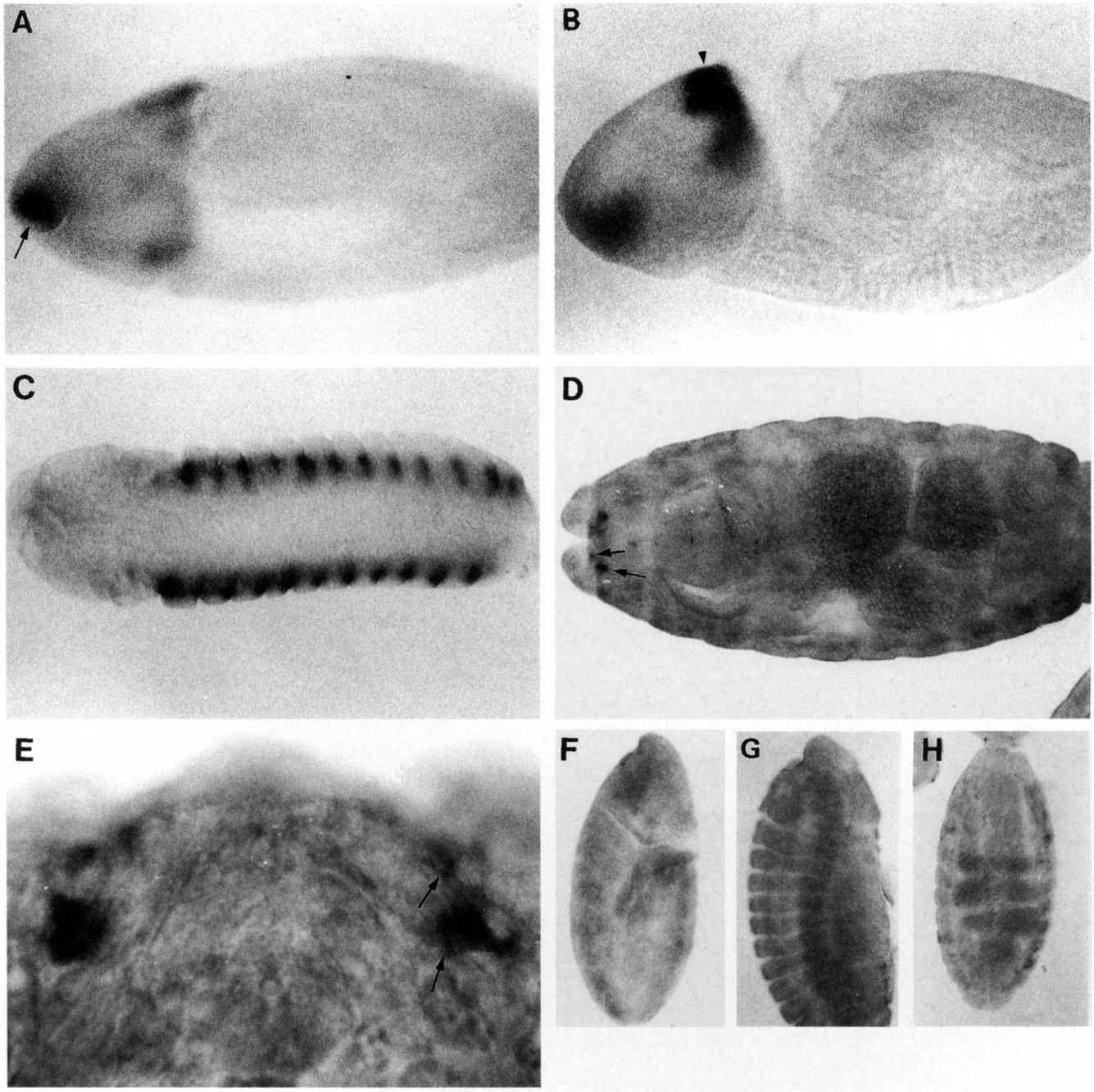

FIGURE 5.—Localization of *so* RNA in embryos. Anterior is to the left in A–D and to the top in E–H. (A) Lateral view of a wild-type embryo showing staining just anterior to the stomadeal invagination (arrow). Magnification, 180×. (B) Lateral view of a wild-type embryo showing cephalic furrow staining (arrowhead). Magnification, 180×. (C) Dorsal view of a stage 12 wild-type embryo showing bilateral staining at all segmental boundaries. Magnification, 180×. (D) Dorsal view of a stage 16 wild-type embryo. Two sets of bilaterally positioned organs are stained in the anterior tip of the embryo (arrows). Magnification, 180×x. (E) Magnified dorsal view of anterior tip staining (arrows) shown in (D). Magnification, 375×. (F) Stage 9 so^{mda} embryo. No staining is detected anterior to the cephalic furrow or anterior to the stomadeal invagination. Magnification, 90×. (G) Stage 12 so^{mda} embryo. *so* RNA is not detected at the segmental boundaries. Magnification, 95×. (H) Stage 16 so^{mda} embryo. There is no detectable *so* RNA in the two pairs of bilaterally positioned organs at the anterior tip of the embryo. Magnification, 90×.

staining pattern of so^{mda} mutant eye disc is identical in pattern and intensity to that of the wild-type discs (Figure 7B). Therefore, the so^{mda} mutation does not affect expression of SO in the eye disc.

SO expression is also detected in adult wild-type and mutant so^{mda} eyes. SO localizes to photoreceptor cell nuclei in the apical regions of the retina which corresponds to the outer photoreceptor cells, R1–6, and the distal central cell, R7 in both wild-type and so^{mda} heads (Figure 7, D and E). In wild-type, SO expression is also detected in the cell nuclei of the optic lobes (Figure 7D). so^{mda} mutant flies do not contain organized optic lobes and

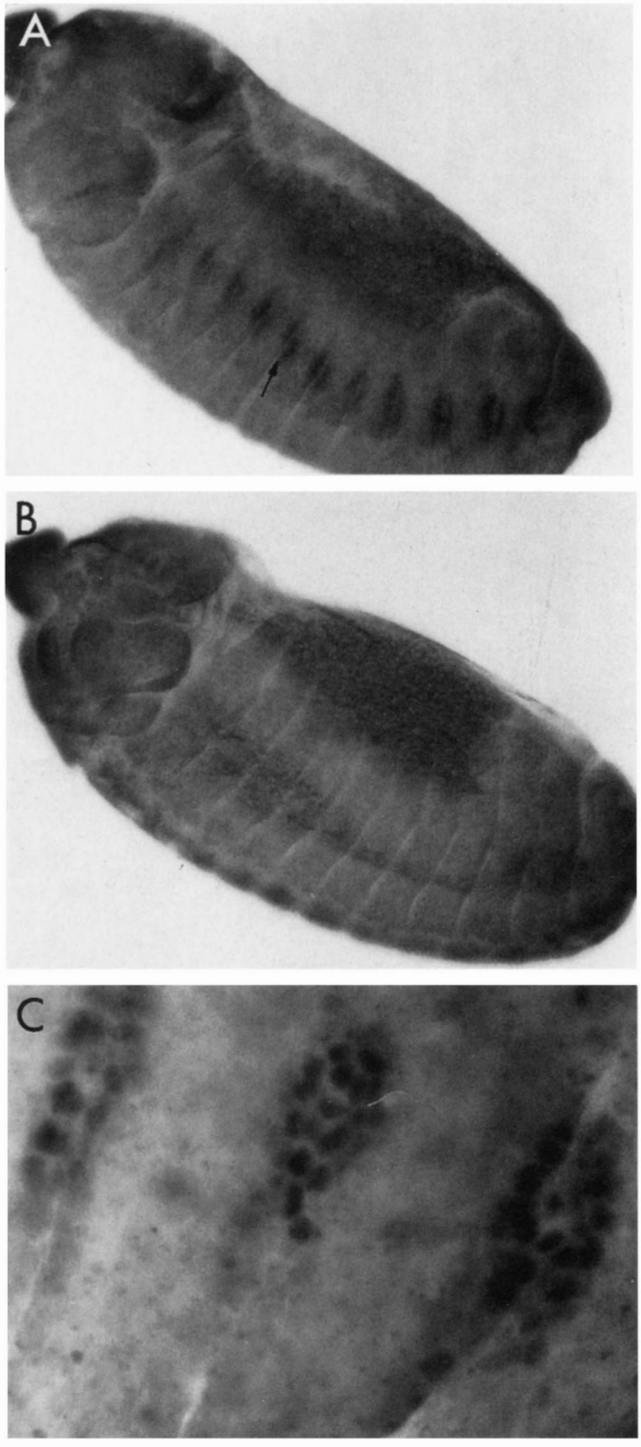

FIGURE 6.—Localization of SO protein in embryos. Anterior is to the left. (A) Stage 12 wild-type embryo showing segmental boundary staining (arrow). Magnification, 180×. (B) Stage 12 so^{mda} embryo. No staining is detected. Magnification, 180×. (C) Magnified view of segmental boundary staining in a wild-type embryo. Magnification, 1050×.

the tissue located in this region does not stain with the SO antisera (Figure 7E). SO protein is also expressed in cell nuclei of the ocelli in wild-type flies (data not shown).

Rescue of the so^{mda} mutant phenotype: To demonstrate that the identified homeodomain gene is solely responsible for the so^{mda} mutant phenotype, the *so* cDNA was placed under the control of the *hsp70* (heat shock protein 70) promoter. This hybrid gene was inserted in the genome of so^{mda} mutant flies by *P* element transformation. Aged embryos were heat shocked at 37° for 1 hr and allowed to mature. Heat pulsing 4–8-hr-old embryos is capable of restoring so^{mda} adults back to a wild-type state. Heat pulsing later in development does not rescue the adult mutant phenotypes.

Rescued flies show a normal adult optic lobe phenotype following expression of *so* in 4–8-hr embryos (see Figure 1G). In addition, these flies exhibit a normal ERG response and do not undergo photoreceptor cell degeneration (data not shown). These results demonstrate that the cloned sequences correspond to the so^{mda} mutation and that the expression of *so* during embryogenesis is sufficient to rescue the adult so^{mda} mutant eye and optic lobe phenotypes.

The same *hsp70/so* hybrid gene was also tested for the ability to rescue the previously isolated so^{1} and so^{2} alleles (HEITZLER *et al.* 1993; LINDSLEY and ZIMM 1992). In these cases, heat shock pulses administered during during eye-antennal imaginal disc development in third instar larva were able to rescue the so^{1} (small eye) and so^{2} (lack of ocelli) mutant defects. These results are consistent with the findings of CHEYETTE *et al.* (1994) and establish that the identified homeobox gene is the *so* gene.

Embryonic and larval defects caused by so^{mda}: Due to the expression of so^{mda} during embryogenesis and the ability to rescue the so^{mda} adult phenotypes during embryogenesis, we examined the defects caused by the so^{mda} mutation earlier in development. so^{mda} embryos do not undergo proper optic lobe invagination. Figure 8 shows representative scanning electron micrographs of stage 12 embryos. Approximately 60% of so^{mda} embryos ($n = 18$) do not show any optic lobe invagination although they appear normal in other aspects of development (Figure 8B). In contrast, so^{1} embryos always properly invaginate the optic lobe area (data not shown). These results indicate that the so^{mda} and so^{1} alleles affect different aspects of *so* function.

In addition, Bolwig's organ and nerve is absent in mutant larva and embryos. Bolwig's organ is visible in stage 16 embryos stained with the neuronal specific antibody MAb22C10. At this stage, Bolwig's organ is located just posterior to the dorsal organ (Figure 8, C and E). Bolwig's nerve runs posteriorly from Bolwig's organ and innervates within an area of the supraesophageal ganglion that will give rise to the optic lobes. The dorsal organ nerve also synapses in this region but at a more dorsal and anterior position than Bolwig's nerve. so^{mda} embryos lack Bolwig's organ and nerve (Figure 8, D and F). In the eye disc, MAb22C10 stains Bolwig's nerve and the developing photoreceptor cells behind the morphogenetic furrow (ZIPURSKY *et al.* 1984). The wild type staining pattern is

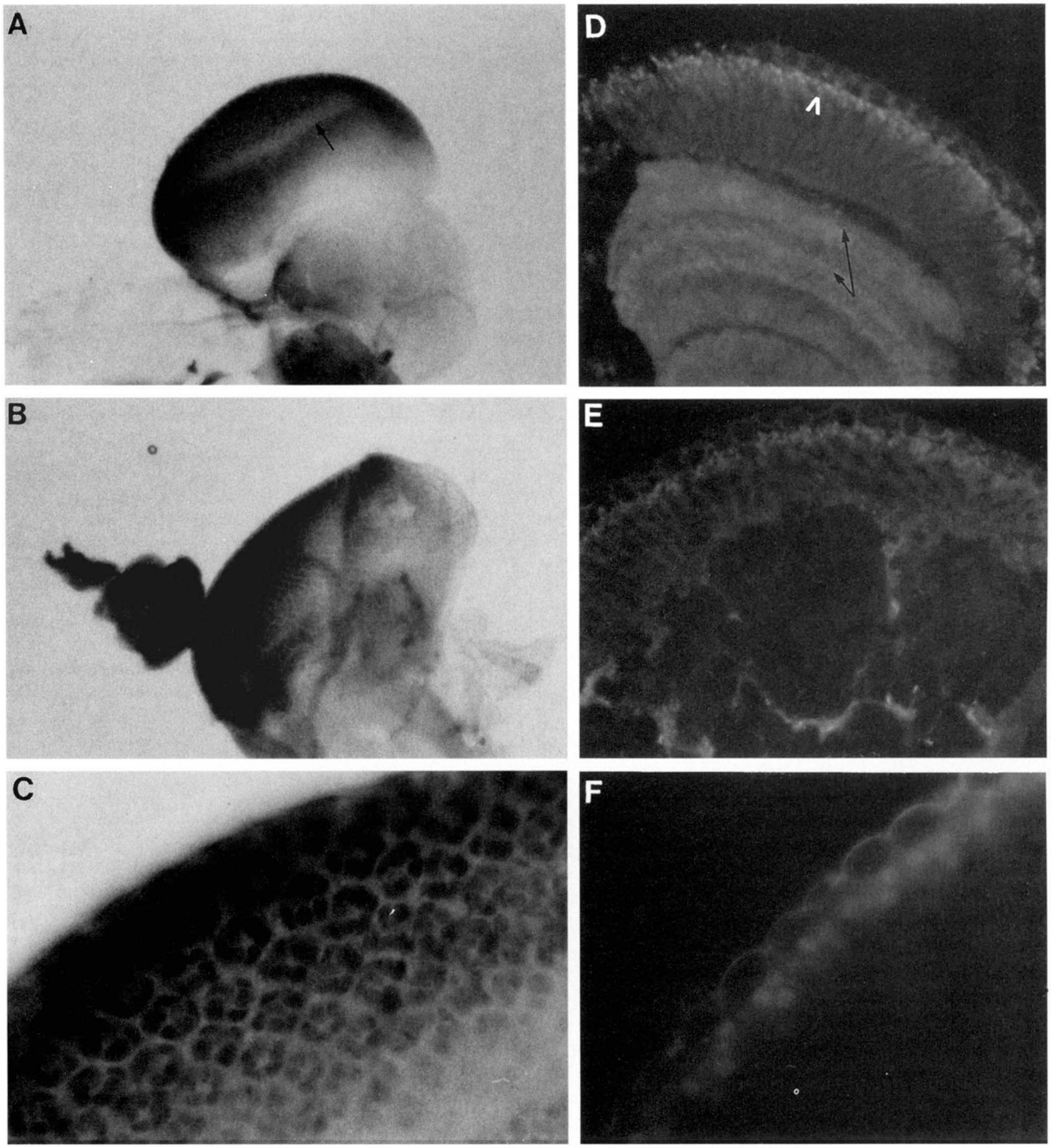

FIGURE 7.—Localization of SO protein in eye-antennal discs and adult heads. (A) Wild-type eye-antennal disc. SO protein is detected posterior to the morphogenetic furrow (arrow) in the developing photoreceptor cells. Staining can also be seen just anterior to the furrow. Magnification, 175×. (B) so^{mda} eye-antennal disc. Disc is abnormal in shape yet stains developing photoreceptor cells. Magnification, 175×. (C) Magnified view of wild-type eye disc. The central cell is not stained as heavily as R1–6 cells. Magnification, 800×. (D) Wild-type adult eye expresses SO in the apical region of the eye (arrowhead) indicating nuclear staining of photoreceptor cells R1–6 and possibly R7. In addition to the eye staining, SO protein is detectable in the optic lobes (arrow). Magnification, 200×. (E) so^{mda} mutant eye shows staining in the apical region of the retina as seen in wild type. The optic lobes of so^{mda} are disorganized and do not stain with the so antiserum. Magnification, 200×. (F) Magnified view of punctate staining of photoreceptor cell nuclei in wild-type eye. Magnification, 600×.

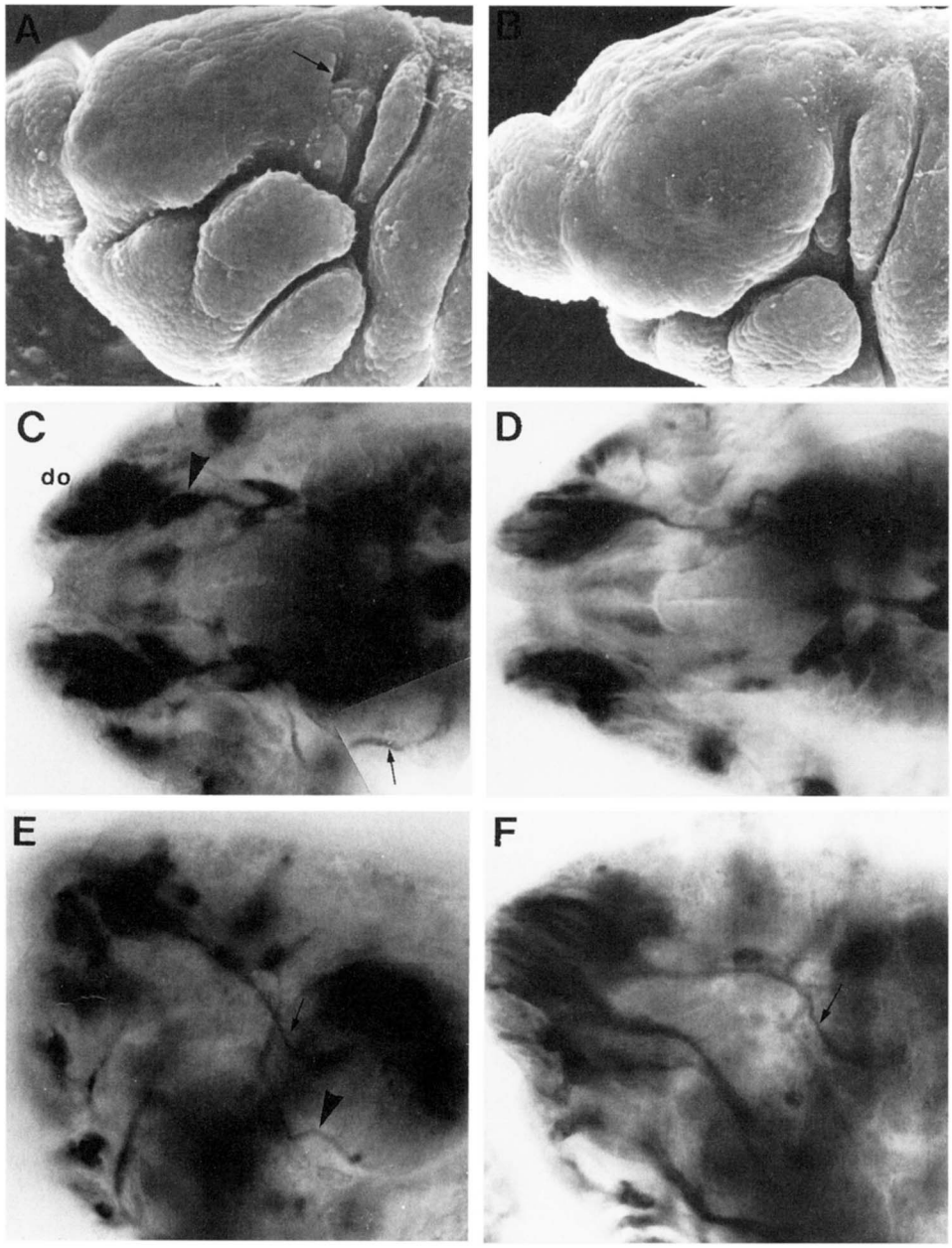

FIGURE 8.—Development of the optic lobe and Bolwig's organ in wild-type and so^{mda} whole mount embryos. Magnification, 500×. (A) Scanning electron micrograph of wild-type embryo showing optic lobe invagination (arrow). (B) so^{mda} embryo lacks optic lobe invagination. Failure to invaginate occurs in 60% of mutant embryos. (C) Embryo stained with the neuronal specific MAb22C10 antibody and viewed with Nomarski optics. Dorsal view of a wild-type stage 12 embryo showing Bolwig's organ (arrowheads) positioned behind to the dorsal organ (do). Bolwig's nerve (arrow) runs posteriorly from Bolwig's organ to its synaptic target in the supraesophageal ganglion (shown in a more ventral plane of focus). (D) Dorsal-ventral view of so^{mda} stage 12 embryo. Bolwig's organ is not present in its normal position near the dorsal organ. Bolwig's nerve is also absent. (E) Lateral view of wild-type embryo. Bolwig's nerve (arrowhead) connects to target cells in the posterior region of the supraesophageal ganglion. The dorsal organ nerve (arrow) synapses with its targets in the anterior region of the ganglion. (F) Lateral view of so^{mda} embryo. Bolwig's nerve is absent (in any plane of focus) although the dorsal organ nerve is visible (arrow).

shown in Figure 9A. Bolwig's nerve runs through the eye disc and optic stalk into the optic lobe anlagen. The other panels of Figure 9 show that so^{mda} discs lack the optic stalk and any physical connection between the developing eye and the brain. As expected, Bolwig's nerve is absent in mutant discs. The mutant discs show a variety of abnormal shapes, but staining of the developing photoreceptor cells is evident in appropriate areas of the discs.

DISCUSSION

A *P* element disrupts the *so* locus: The *so* gene was cloned by *P* element tagging. Two lines of evidence indicate that the mutant phenotype of so^{mda} is caused by loss of this gene function. First, the *P* element responsible for the so^{mda} mutation is located within the 5′-noncoding region of the *so* gene, and therefore is expected to disrupt the expression or maturation of this mRNA. This expectation was verified by *in situ* hybridization studies, in which no *so* mRNA could be detected in mutant embryos. A second, more stringent, test came from analysis of so^{mda} flies bearing a heat shock promoter/*so* cDNA gene fusion. Ubiquitous expression of the wild-type *so* gene during embryogenesis rescues the so^{mda} mutant phenotype. We have not found a dominant gain of function phenotype associated with ectopic expression of the *so* gene.

Structure of the SO protein: Homeodomain proteins have been organized into classes based on amino acid conservation within the homeodomain (TREISMAN *et al.* 1992). The SO homeodomain is a member of the bicoid class because it contains a lysine at homeodomain position 50. Of the numerous Drosophila homeodomains

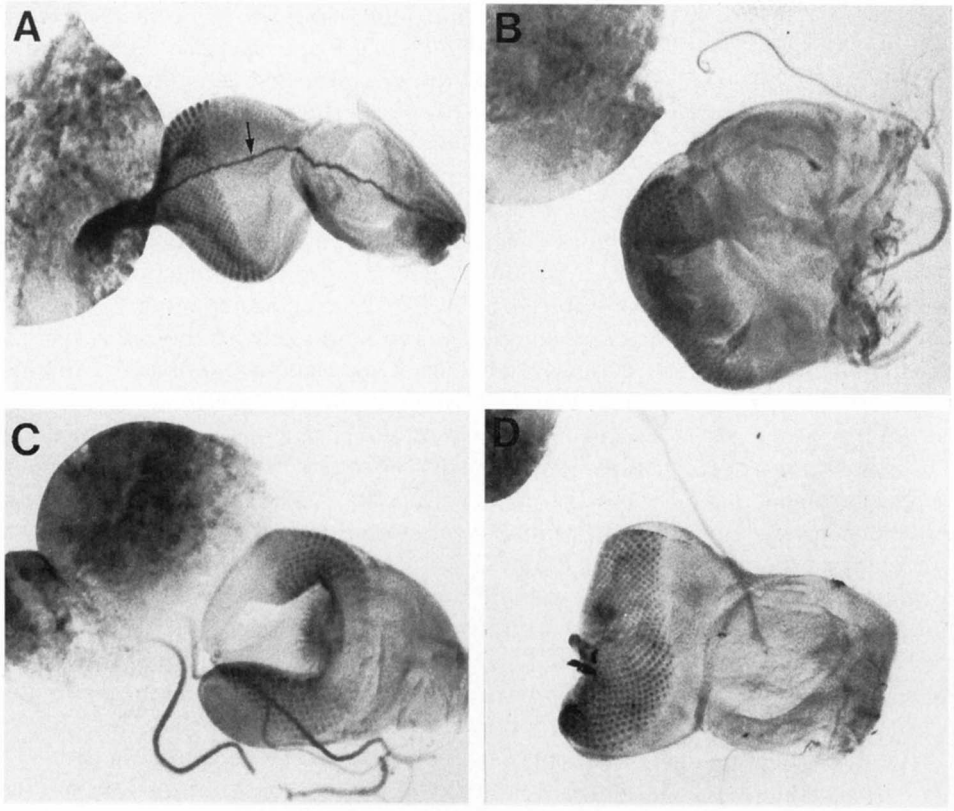

FIGURE 9.—Development of the eye-antennal imaginal disc in wild-type and so^{mda} larva. Magnification, 100×. (A) Whole mount preparation of a wild-type disc stained with MAb22C10. Bolwig's nerve (arrow) and the developing photoreceptor cell bodies posterior to the morphogenetic furrow are stained. The axons of the photoreceptor cells, also stained, follow Bolwig's nerve through the optic stalk, into the developing optic lobes within the brain hemisphere. (B and C) so^{mda} discs stained with MAb22C10. Mutant discs lack an optic stalk and are abnormal in overall shape. The photoreceptor cell bodies are stained, but Bolwig's nerve is absent and photoreceptor axons fail to innervate the brain. These two micrographs provide examples of the abnormal morphology present in the so^{mda} disc. (D) In rare cases, a stump probably representing a rudimentary optic stalk is seen in mutant eye discs. Still, Bolwig's nerve cannot be detected.

previously studied, only bicoid, orthodenticle, and Pem contain a lysine at this position. Most other known homeodomains contain a glutamine or serine. TREISMAN *et al.* (1989) showed that changing this single amino acid, the serine at position 50 to a lysine in the paired homeodomain, allowed the protein to bind the *bicoid* consensus binding site where it originally could not. Studies in yeast (HANES and BRENT 1991) and in the Schneider Drosophila cell line (TREISMAN *et al.* 1992) have given similar results implicating amino acid 50 as a major determinant in binding specificity. Studies using this sequence can give clues as to the binding capabilities of SO and may be helpful in identifying target genes that SO may regulate.

The SO homeodomain is distinct from other homeodomains in that it lacks two highly conserved amino acids, an arginine at position 5 and a glutamine at position 12 in the homeodomain. The arginine at position 5 is in the non-helical region at the N terminus and is conserved in 97% of the homeodomians isolated (KORNBERG 1993). This residue contacts base pairs in the TAAT target core as the N-terminal arm makes contact with the minor groove of the DNA double helix (TREISMAN *et al.* 1992). The glutamine at position 12 is part of helix 1. The absence of these amino acids may indicate a novel structure within the N-terminal region of the homeodomain that would affect the binding capability of the SO homeodomain. Also, the SO homeodomain is one of the few homeodomains distributed over three exons instead of being contained in one exon (POOLE *et al.* 1985).

***so* is expressed at invagination areas in the embryo:** *so* is expressed at various stages and locations in the wild-type embryo. A common theme is that *so* is found at areas of invagination; immediately anterior to the cephalic furrow and stomadeal invagination in stage 9 embryos and at segmental boundaries in stage 12 embryos. If *so* expression is a component of a developmental pathway specifying proper infolding of ectodermal tissue during cell migration, mutant phenotypes could be traced back to such invagination defects during embryogenesis. We have limited data indicating such defects. First, the so^{mda} eye-antennal imaginal discs, which arise from modified invaginations of the epidermis (POODRY 1980), are aberrant in shape. Second, so^{mda} embryos fail to invaginate properly at the optic lobe region. Third, Bolwig's organ itself, which is missing in *so* mutants, is formed via the same invagination as the optic lobe (GREEN *et al.* 1993). We have not observed other morphogenetic problems despite the expression of so at other sites of invagination. This is likely due to the hypomorphic nature of the so^{mda}. Null mutations in the *so* gene are known to cause lethality (HEITZLER *et al.* 1993) consistent with the role of *so* during embryonic morphogenesis.

The phenotype of so^{mda} mutants: Several genes have been implicated in Bolwig's organ and nerve development. The disconnected (*disco*) gene is involved in the pathfinding of Bolwig's nerve (STELLER *et al.* 1987). Bolwig's nerve grows normally but is unable to recognize its target cells. The *glass* mutation affects the

fasiculation of the Bolwig's axons to the pioneer axon and the directed outgrowth of the nerve (MOSES *et al.* 1989). *Kruppel* affects the differentiation of neurons into Bolwig's organ, the maintenance of fasiculation of Bolwig's axons, and the routing of the nerve to its synaptic targets in the brain (SCHMUCKER *et al.* 1992). We have not observed remnants of Bolwig's organ or nerve in so^{mda} as seen in *disco*, *glass* and *Kruppel* which suggests that *so* action precedes the action of these genes in Bolwig's nerve development. This is consistent with the observation that the process of optic lobe invagination, which occurs earlier in embryonic development than the specification of Bolwig's organ and nerve, is faulty in so^{mda}.

Examination of third instar larval eye imaginal discs confirm that Bolwig's nerve is absent in so^{mda} mutants. These discs are abnormal in shape and lack an optic stalk. Therefore, no innervation of the larval brain can take place by the developing photoreceptor cells of the compound eye. The lack of retinal innervation in the third instar larval period leads to mutant phenotypes in the adult fly: aberrant optic lobe development, external eye defects, depleted response to a light stimulus, age-dependent retinal degeneration. Proper optic lobe development strictly depends on retinal innervation (MEYEROWITZ and KANKEL 1978; POWER 1943; SELLECK and STELLER 1991). Studies have shown that normal retinal development can proceed irrespective of optic lobe abnormalities however, the optic lobes cannot form properly if photoreceptor cell axons do not arrive at proper optic lobe targets. SELLECK and STELLAR (1991) further showed that mitotically active lamina precursor cells are absent in mutants that lack retinal innervation. They conclude that photoreceptor cell innervation is necessary to initiate precursor cell division to produce lamina neurons. In light of these results, it is not surprising that optic lobe structures do not develop appropriately in so^{mda} mutants. so^{mda} mutants also display external defects in the eye. The roughness of so^{mda} eyes is not caused by aberrant ommatidial shapes and sizes as seen in other rough eye mutants (MEYEROWITZ and KANKEL 1978). Instead, the roughness is caused by indentations in the eye presumably due to structural defects in the underlying optic lobes.

so^{mda} mutants show a drastically depleted response to a light stimulus as measured by an ERG. This phenotype is present in newly eclosed so^{mda} flies, before the onset of retinal degeneration. We favor the hypothesis that so^{mda} flies show a deficient ERG due to the structural abnormalities of the basement membrane and optic lobes. These structures are known to have low conductivity (HEISENBERG 1971) and to allow the retina to be electrically isolated from the rest of the head. For this reason, a large voltage response can be measured in the electroretinogram. When this membrane is disturbed, the measured voltage would be significantly less. Therefore, the ERG defect in so^{mda}, which typically signifies a phototransduction defect, could be a secondary effect of the structural defects of the optic ganglia. The *disco* mutants that show the disconnected phenotype and lack optic lobe structures also show a similar ERG response to so^{mda} flies (CAMPOS *et al.* 1992).

so^{mda} photoreceptor cells show age-dependent retinal degeneration. Previous work has shown that photoreceptor cell terminal differentiation can occur in the absence of retinal innervation, but maintenance of mature photoreceptor cells after eclosion requires proper neural connections to target cells of the optic ganglia (CAMPOS *et al.* 1992). Our results are consistent with this view. The so^{mda} adult phenotypes are very similar to those seen in the *disco* mutants that show an unconnected phenotype. The unconnected disco mutants lack proper Bolwig's nerve connection to the embryonic brain and show retinal degeneration (CAMPOS *et al.* 1992; STELLER *et al.* 1987).

The role of Bolwig's nerve in pathfinding: Bolwig's nerve runs through the eye-antennal disc, through the optic stalk, and into the brain in wild-type third instar larva. The developing photoreceptor cells project axons along side Bolwig's nerve through the stalk and synapse at target cells in the optic lobes. We show that the so^{mda} mutation prevents photoreceptor cells from innervating proper optic lobe target cells in the brain of third instar larva. The most prominent defect in the so^{mda} disc is the absence of an optic stalk which prevents any physical connection between the eye and the brain.

STELLER *et al.* (1987) postulated that adult photoreceptor cells follow a pioneer pathway created by Bolwig's nerve when innervating the third instar larval brain. When Bolwig's nerve development is abnormal (as shown previously for *disco* and now for so^{mda}), adult photoreceptor cells fail to synapse at proper target cells in the brain. These results are consistent with the idea that Bolwig's nerve directs retinal cell axons to their proper destinations in the brain. More recent evidence has challenged this view. KUNES and STELLER (1991) have shown that toxin mediated ablation of Bolwig's nerve during pupal development has no effect on retinal cell axon projections. In addition, KUNES *et al.* (1993) have shown that $glass^{+}$ patches of retinal tissue can project axons to their proper locations in the absence of Bolwig's nerve.

If Bolwig's nerve is not needed to direct retinal cell axons, then *so* must affect other larval visual system elements that are involved in the axonal pathfinding of adult retinal cells. Since optic lobe development is disrupted in so^{mda} mutants, the optic lobe may fail to present a recognizable target for the developing photoreceptors of the imaginal disc. A second possibility is that specification of Bolwig's organ is developmentally related to the specification of the adult optic pathway. Developmental mutations such as so^{mda} and *disco* may affect both processes. In either case, our results show that the elements of the adult photoreceptor axonal

pathway is established during embryonic development, and the activity of the *so* gene is required for this process.

Role of the SO gene product: We have focused on the role of the *so* gene during the specification of the larval photoreceptor system and its affect on the adult visual system because this process is affected by the so^{mda} allele. *so* encodes a homeodomain protein that likely plays a role in transcriptionally regulating genes necessary for proper optic lobe invagination and Bolwig's organ formation during embryogenesis. The expression pattern of the *so* gene suggest that it is involved in additional roles during embryonic development, perhaps all sharing the common theme of cell movement during morphogenesis.

Although so^{mda} and so^{1} are alleles of the same gene, they show full genetic complementation. We have shown that the so^{mda} *P*-element mutation affects only embryonic expression. The *P* element location in the so^{mda} allele does not affect the coding capacity of the gene. This suggests that this mutation disrupts a regulatory region needed for proper embryonic expression. The results of CHEYETTE *et al.* (1994) show that the so^{1} mutation affects only adult expression of the *so* gene. These results likely explain the complementation of the so^{mda} and so^{1} alleles in genetic tests: so^{mda} providing embryonic SO product and so^{1} providing adult visual system product. The allelic nature of so^{mda} and so^{1} is supported by ability of the hsp70/cDNA construct to rescue both mutations. In addition, the time needed for induction of the SO product from this construct, early for so^{mda} and late for so^{1} fits in well with the model that so^{mda} affects early expression and so^{1} affects late expression. Analysis of each class of *so* alleles establishes a role of *so* in both specification of larval photoreceptor development during embryogenesis and in morphogenesis of the adult eye that begins during the third instar larval period.

We thank BILL ARCHER and SHEILA ADAMS for histology work; SEYMOUR BENZER, TADMIRI VENKATESH and HUGO BELLEN for providing antibodies; REGGIE HO for initial characterization of the *so* ERG; FINTAN STEELE for help on *in situ* hybridizations; PHIL YODER for assistance with DNA sequencing; and BENJAMIN CHEYETTE, PATRICIA GREEN and LAWRENCE ZIPURSKY for sharing data prior to publication. This work was supported by grant NEIEY06808 from National Institutes of Health to J.E.O.

LITERATURE CITED

ASHBURNER, M., 1989 *Drosophila: A Laboratory Handbook.* Cold Spring Harbor Laboratory, Cold Spring Harbor, N.Y.

BOLWIG, N., 1946 Sense and sense organs of the anterior end of the housefly larvae. Vidensk. Medd. Dan. Naturhist. Foren. **109:** 81–217.

BREIER, G., G. R. DRESSLER and P. GRUSS, 1988 Primary structure and developmental expression pattern of *Hox 3.1*: a member of the murine *Hox 3* homeobox gene cluster. EMBO J. **7:** 1329–1336.

CAMPOS, A., K. F. FISCHBACH and H. STELLER, 1992 Survival of photoreceptor neurons in the compound eye of *Drosophila* depends on connections with the optic ganglia. Development **114:** 355–366.

CAVENER, D. R., 1987 Comparison of the consensus sequence flanking translational start sites in *Drosophila* and vertebrates. Nucleic Acids Res. **15:** 1353–1361.

CHEYETTE, B., P. GREEN, K. MARTIN, H. GARREN, V. HARTENSTEIN *et al.*, 1994 The Drosophila *sine oculis* locus encodes a homeodomain-containing protein required for the development of the entire visual system. Neuron **12:** 977–996.

DRIEVER, W., and C. NUSSLEIN-VOLHARD, 1989 The Bicoid protein is a positive regulator of *hunchback* transcription in the early *Drosophila* embryo. Nature **337:** 138–143.

FLEGEL, W. A., A. W. SINGSON, J. S. MARGOLIS, A. G. BANG, J. W. POSAKONY *et al.*, 1993 *Dpbx*, a new homeobox gene closely related to the human proto-oncogene *pbx1* Molecular structure and developmental expression. Mech. Dev. **41:** 155–161.

GREEN, P., A. Y. HARTENSTEIN and V. HARTENSTEIN, 1993 The embryonic development of the Drosophila visual system. Cell Tissue Res. **273:** 583–598.

HANES, S. D., and R. BRENT, 1991 A genetic model for interaction of the homeodomain recognition helix with DNA. Science **251:** 426–430.

HEISENBERG, M., 1971 Separation of receptor and lamina potentials in the electroretinogram of normal and mutant Drosophila. J. Exp. Biol. **55:** 85–100.

HEITZLER, P., D. COULSON, M. T. SAENZ-ROBLES, M. ASHBURNER, J. ROOTE *et al.*, 1993 Genetic and cytogenetic analysis of the 43A-E region containing the segment polarity gene costa and the cellular polarity genes prickle and spiny-legs in *Drosophila melanogaster.* Genetics **135:** 105–115.

ITOH, N., P. SALVATERRA and K. ITAKURA, 1985 Construction of an adult Drosophila head cDNA expression library with lambda gt 11. Drosophila Inf. Serv. **61:** 89.

KORNBERG, T., 1993 Understanding the homeodomain. J. Biol. Chem. **268:** 26813–26816

KUNES, S., and H. STELLAR, 1991 Ablation of Drosophila photoreceptor cells by conditional expression of a toxin gene. Genes Dev. **5:** 970–983.

KUNES, S., C. WILSON and H. STELLER, 1993 Independent guidance of retinal axons in the developing visual system of Drosophila. J. Neurosci. **13:** 752–767.

LARRIVEE, D., S. CONRAD, R. STEPHENSON and W. PAK, 1981 Mutation that selectively affects Rhodopsin concentration in the peripheral photoreceptors. J. Gen Physiol. **78:** 521–545.

LINDSLEY, D., and ZIMM, 1992 *The Genome of Drosophila melanogaster.* Academic Press, San Diego.

MANIATIS, T., R. HARDISON, E. LACY, J. LAUER, C. O'CONNELL *et al.*, 1978 The isolation of structural genes from libraries of eukaryotic DNA. Cell **15:** 687–701.

MEYEROWITZ, E., and D. KANKEL, 1978 A genetic analysis of visual system development in *Drosophila melanogaster.* Dev. Biol. **62:** 112–142.

MOSES, K., M. ELLIS and G. RUBIN, 1989 The *glass* gene encodes a zinc-finger protein required by *Drosophila* photoreceptor cells. Nature **340:** 531–536.

POODRY, C. A., 1980 *The Genetics and Biology of Drosophila*, pp. 407–432, edited by M. ASHBURNER and T. R. F. WRIGHT. Academic Press, New York.

POOLE, S., L. KAUVAR, B. DREES and T. KORNBERG, 1985 The engrailed locus of Drosophila: structural analysis of an embryonic transcript. Cell **40:** 37–43.

POWER, 1943 The effect of reduction in numbers of ommatidia upon the brain of *Drosophila melanogaster.* J. Exp. Zool. **94:** 33–71.

READY, D. F., 1989 A multifaceted approach to neural development. Trends Neurosci. **12:** 102–110.

REGULSKI, M., K. HARDING, R. KOSTRIKEN, F. KARCH, M. LEVINE *et al.*, 1985 Homeo box genes of the Antennapedia and Bithorax complexes of Drosophila. Cell **43:** 71–80.

ROBERTSON, H., C. PRESTON, R. PHILLIS, D. JOHNSON-SCHLITZ, W. BENZ *et al.*, 1988 A stable genomic source of *P* element transposase in *Drosophila melanogaster.* Genetics **118:** 461–470.

RUBIN, G., 1991 Signal transduction and the fate of the R7 photoreceptor in Drosophila. Trends Genet. **7:** 372–377.

RUBIN, G., and A. SPRALDING, 1982 Genetic transformations of Drosophila with transposable element vectors. Science **218:** 348–353.

SCHMUCKER, D., H. TAUBERT and H. JACKLE, 1992 Formation of the *Drosophila* larval photoreceptor organ and its neuronal differentiation require continuous *Kruppel* gene activity. Neuron **9:** 1025–1039.

SCHNEUWLY, S., R. KLEMENZ and W. GEHRING, 1987 Redesigning the body plan of Drosophila by ectopic expression of the homeotic gene *Antennapedia*. Nature **325:** 816–818.

SELLECK, S., and H. STELLER, 1991 The influence of retinal innervation on neurogenesis in the first optic ganglion of *Drosophila*. Neuron **6:** 83–99.

SMITH, D. B., and K. S. JOHNSON, 1988 Single-step purification of polypeptides expressed in *Escherichia coli* as fusions with glutathione *S*-transferase. Gene **67:** 31–40.

SMITH, D. B., K. M. DAVERN, P. G. BOARD, W. U. TIU, E. G. GARCIA *et al.*, 1986 M_r 26,000 antigen of *Schistosoma japonicum* recognized by resistant WEHI 129/J mice is a parasite glutathione *S*-transferase. Proc. Natl. Acad. Sci. USA **83:** 8703–8707.

STELLER, H., K. F. FISCHBACH and G. RUBIN, 1987 *disconnected*: a locus required for neuronal pathway formation in the visual system of *Drosophila*. Cell **50:** 1139–1153.

TAUTZ, D., and C. PFEIFLE, 1989 A non-radioactive *in situ* hybridization method for the localization of specific RNAs in *Drosophila* embryos reveals translational control of the segmentation gene *hunchback*. Chromosoma **98:** 81–85.

TIX, S., J. MINDEN and G. TECHNAU, 1987 Pre-existing neuronal pathways in the developing optic lobes of Drosophila. Development **105:** 739–746.

TOMLINSON, A., B. KIMMEL and G. RUBIN, 1988 *rough*, a Drosophila homeobox gene required in photoreceptors R2 and R5 for inductive interactions in the developing eye. Cell **55:** 771–784.

TREISMAN, J., P. GONCZY, M. VASHISHTHA, E. HARRIS and C. DESPLAN, 1989 A single amino acid can determine the DNA binding specificity of homeodomain proteins. Cell **59:** 553–562.

TREISMAN, J., E. HARRIS, D. WILLSON and C. DESPLAN, 1992 The Homeodomain: a new face for the helix-turn-helix? Bioessays **14:** 145–150.

WHARTON, K., B. YEDVOBNICK, V. FINNERTY and S. ARTAVANIS-TSAKONAS, 1985 Opa: a novel family of transcribed repeats shared by the *Notch* locus and other developmentally regulated loci in D. melanogaster. Cell **40:** 55–62.

ZIPURSKY, C. S., T. R. VENKATESH, D. B. TEPLOW and S. BENZER, 1984 Neuronal development in the Drosophila retina: monoclonal antibodies as molecular probes. Cell **36:** 15–26.

Communicating editor: T. W. CLINE